Hybrid Power Bank Deployment Model for Energy Supply Coverage Optimization in Industrial Wireless Sensor Network

Hang Yang[1,2,*], Xunbo Li[1] and Witold Pedrycz[2]

[1]School of Mechanical and Electrical Engineering, University of Electronic Science and Technology of China, Chengdu, Sichuan, 611731, China
[2]Department of Electrical and Computer Engineering, University of Alberta, Edmonton, AB T6G 1H9, Canada
*Corresponding Author: Hang Yang. Email: hang.yang@outlook.com

Abstract: Energy supply is one of the most critical challenges of wireless sensor networks (WSNs) and industrial wireless sensor networks (IWSNs). While research on coverage optimization problem (COP) centers on the network's monitoring coverage, this research focuses on the power banks' energy supply coverage. The study of 2-D and 3-D spaces is typical in IWSN, with the realistic environment being more complex with obstacles (i.e., machines). A 3-D surface is the field of interest (FOI) in this work with the established hybrid power bank deployment model for the energy supply COP optimization of IWSN. The hybrid power bank deployment model is highly adaptive and flexible for new or existing plants already using the IWSN system. The model improves the power supply to a more considerable extent with the least number of power bank deployments. The main innovation in this work is the utilization of a more practical surface model with obstacles and training while improving the convergence speed and quality of the heuristic algorithm. An overall probabilistic coverage rate analysis of every point on the FOI is provided, not limiting the scope to target points or areas. Bresenham's algorithm is extended from 2-D to 3-D surface to enhance the probabilistic covering model for coverage measurement. A dynamic search strategy (DSS) is proposed to modify the artificial bee colony (ABC) and balance the exploration and exploitation ability for better convergence toward eliminating NP-hard deployment problems. Further, the cellular automata (CA) is utilized to enhance the convergence speed. The case study based on two typical FOI in the IWSN shows that the CA scheme effectively speeds up the optimization process. Comparative experiments are conducted on four benchmark functions to validate the effectiveness of the proposed method. The experimental results show that the proposed algorithm outperforms the ABC and gbest-guided ABC (GABC) algorithms. The results show that the proposed energy coverage optimization method based on the hybrid power bank deployment model generates more accurate results than the results obtained by similar algorithms (i.e., ABC, GABC). The proposed model is, therefore, effective and efficient for optimization in the IWSN.

1 Introduction

With the rapid development of modern manufacturing, there is a shift from simple production to intelligent production. Since the factory has its complexity and needs to keep its originality of guaranteeing the running of the production line, adding a traditional cable network is not advisable. The wiring could interfere with the existing process and require the production line to be transformed into a new factory. Thus, there is a high demand for IWSN-enabled intelligent production, which helps monitor the manufacturing process and sets actual databases for future upgrades. Various IWSN applications require deploying different sensor devices to monitor the production line for other purposes. Since the sensor devices must operate and monitor continuously, the power supply becomes a limitation; powering the sensor devices with batteries requires future replacement, recharging, and maintenance, which is not convenient and may miss the detection of some typical parameters. With the booming expansion of efficient printing circuits and the fabrication of highly-integrated devices, the application of powering devices by radio-frequency (RF) is essential for inspiring the use of RF-enabled sensor devices in industries.

Regarding energy harvesting, the sensor devices can only harvest energy within a certain distance from the power banks. The power banks are equipped with grid power and can send RF signals at a fixed capacity. The hybrid power bank operates on RF and uses it to propagate energy to the devices in the deployment area. Many existing works in the literature assumed the range as a circle with a fixed radius, ignoring the influence of the ambient environment and deviating from reality. In contrast, we propose a probabilistic model which improves the accuracy of the harvest range, taking into consideration the influence of obstacles in the environment. Particularly in terms of the geometric plane distance, we focus on the interference of the RF signal from the three-dimensional (3-D) surface. Generally, there exist machines, semi-finished products, carrier boxes, pieces of furniture, and operators in the production line, and they all interfere with the RF signal to the degree that cannot be ignored.

The topic of energy supply coverage has quickly become one of the most attractive variables determining the quality of service in IWSNs. The power bank can serve the sensor devices within their coverage range while all current sensor devices, FOI, and coverage areas are known. Due to the dynamic nature of IWSN, and the sensor devices being self-configurable and able to be online automatically and opportunistically, it is possible to target the overall energy supply coverage. Because the power banks are always online and the interference of the RF signal is dynamic, the coverage rate of a particular point is not deterministic but based on presumptions. However, once a sensor device of the IWSN is deployed, the coverage probability can be determined according to its physical location following the hybrid power bank deployment model. The purpose of studying the energy supply coverage is to find the optimal least number of power banks which not only powers the current sensor devices but also reserve redundancy for the future development of IWSN while guaranteeing the operation of the IWSN.

In the IWSN, coverage, connectivity, and routing are the typical factors to be considered. We focus on the power supply coverage of the IWSN in this research work. The minimum number of power

banks and their deployment locations is determined before the deployment of the sensor devices and running the IWSN. If any sensor device fails to be under the coverage area of the power banks, it will not function properly and be disconnected from its application network. Thus the IWSN fails to accomplish its task. In this research work, we first plot the 3-D surface of the application FOI, and then deploy some of the power banks and check the power supply coverage rate of each point on the FOI. Because there exist coverage cavities, there is a need to add more power banks to fill them and calculate the power supply coverage of each point. The newly added power banks cover the coverage cavities and enhance the coverage rate of the areas around the cavities.

With all the analyses above, two critical issues arise. 1) How to mimic the real FOI and compute their coverage rate. 2) How to find the coverage cavities and fill them. First, we propose establishing a 3-D projecting model and the probabilistic model to better reflect RF signal status at the point on the 3-D surface. Second, the wavelet sub-band energy entropy is utilized with metaheuristics methods to find the cavities and decide where to deploy the new power banks, thus improving the overall coverage.

This research work lies in artificial intelligence, modelling, and systems engineering, focusing on the coverage rate of the specific targets or the target areas but expanding the scenarios in work to a broader range. The presumable coverage rate of every point on the FOI and the coverage rate of the targets or the target areas can be derived accordingly. While much of the existing research treats the FOI as a 2-D plane or 3-D space, we draw from practice that it is a 3-D surface, the power banks can only be deployed on the surface, and the RF signals cannot penetrate the surface. As illustrated in Fig. 1, treating the FOI directly as a 2-D ideal plane will ignore the coverage cavities. Hence, the proposed hybrid power bank deployment model is effective due to its flexibility for newly established plants and plants already deployed with some IWSN systems.
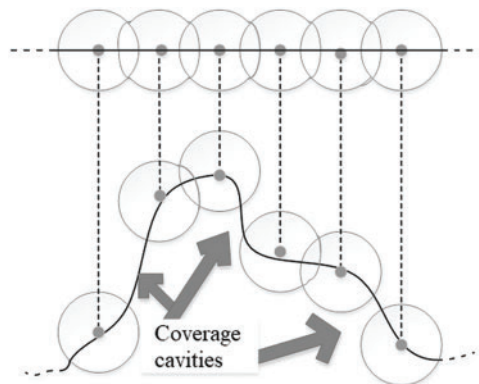
**Figure 1:** A 2-D plane showing coverage cavities in a practical application

In Fig. 1, the coverage cavities are shown in real-life applications where the deployment is implemented considering each power bank's obstacles and coverage area.

The main contribution of this research work is given as follows:

- Design and implementation of a hybrid metaheuristics algorithm for coverage optimization.
- The FOI settings in the model are tunable, and the interferences are transferred to obstacles of the 3-D surface, which fluctuate the terrain.
- The traditional 2-D Bresenham's algorithm [1] was extended to 3-D for line-of-sight (LOS) or non-line-of-sight (NLOS) determining of points on 3-D surfaces.

- The traditional artificial bee colony (ABC) algorithm is employed with a dynamic search strategy (DSS) for the NP-hard deployment problem. It balances the global and local search ability and cellular automata to accelerate the convergence speed, thus resulting in a better and quicker solution for power bank deployment locations.
- The comparative experiments on numerical benchmark function optimization are carried out for the artificial bee colony with a dynamic search strategy (ABC-DSS) algorithm compared to the ABC and GABC algorithms, verifying that the proposed algorithm is competitive.

The overall flow of the hybrid power bank deployment model is given in Fig. 2.
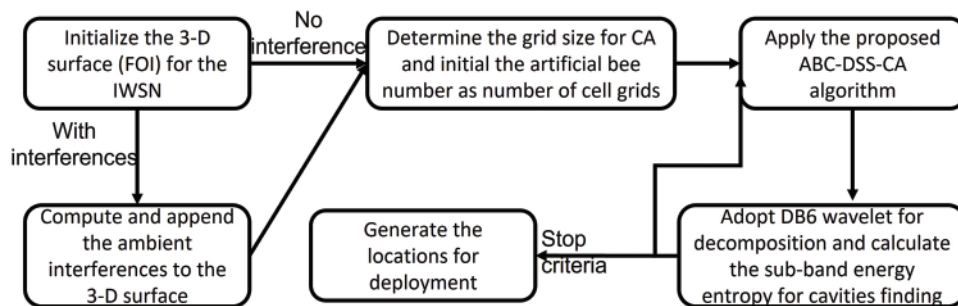
Figure 2: Overall flow of the hybrid power bank deployment model

Wireless sensor networks (WSN) are currently used in several applications, such as environmental monitoring, military surveillance, and smart cities [2–4]. Researchers have studied the COP of WSN for years w.r.t. 2-D plane [5–12], 3-D space [13–16], and 3-D terrain [17–19]. Since the sensing region of the sensors on the 2-D plane can be simplified as a disk with the deployment location as the center, the researchers used mathematical calculations to resolve the COP [7,8,12]. Note that the researchers all consider the single sensor coverage region as omnidirectional in the 2-D plane, and the directional type sensor was adopted in [13,14], a heuristic algorithm was utilized in [14], and a pyramid shape sensing type was adopted in [13]. The sensor deployment method in 3-D terrain utilized the heuristic algorithm to conquer the COP and adopted a cone-ball-shaped sensing model for precision [17,19]. There are other heuristic algorithms utilized for targeting COP issues in the literature, such as the marine predator algorithm [11], the Yin-Yang pigeon-inspired optimization algorithm [20], and the whale optimization algorithm [21].

In this paper, we study the COP of IWSN. Since the birth of the IWSNs, the network performance has been tied closely to the ambient environment or the ambient wireless conditions, especially in industrial applications. Precisely, we deploy the power banks on a 3-D surface, which not only takes the shape of the geometry terrain but also appends the interference from the ambient environment to the 3-D surface. Approximation algorithms are efficient algorithms that find approximate solutions to optimization problems (in particular NP-hard problems) with provable guarantees on the distance of the returned solution to the optimal one [22]. In setting the fundamentals of our future research, we first need to guarantee the coverage of the power supply network to maintain the energy supplement. The coverage issues can be classified roughly based on the type of solving methodology, utilizing the scheme based on the classical methods and the scheme based on metaheuristic methods. While the COP problem in the 2-D plane can be seen as a traditional art gallery problem, it becomes NP-hard when extended to 3-D space, 3-D terrain, and 3-D surface. The art gallery problem originates from a real-world problem of minimizing the number of guards guarding an art gallery, which can be optimally resolved in polynomial time [20,23]. For NP-hard problems, while inspired by genetic

and biological intelligence, most heuristic methods are advanced and optimized to accomplish a particular task when the traditional mathematic methods are not appropriate. The original and greedily mentioned heuristics methods include genetic algorithms (GA) by Holland in 1992 [24], particle swarm optimization (PSO) by Eberhart and Kennedy in 1995 [25], artificial bee colony(ABC) by Karaboga in 2005 [26], ant colony optimization (ACO) by Dorigo and Blum in 2005 [27], and simulated annealing (SA) by Kirkpatrick et al. in 1983 [27,28], and differential evolution (DE) by Price et al. in 2006 [29]. Other researchers also modified or extended the original type and derived many new methods or solutions. Many comparative experiments on numerical benchmark function optimization were conducted for ABC in [26,30–32], and the experimental results reveal that ABC is competitive over some conventional heuristic optimization methods, such as GA [24,33], DE [29,34], and PSO [25,35]. Thus, in this work, we utilize three ABCs, the traditional ABC algorithm, the GABC algorithm [36], and the proposed ABC-DSS algorithm, which addresses the COP.

Several approximation algorithms and methods have been utilized in the literature for the covering models. The sensing models can be either deterministic or probabilistic. We assume the average covering range is r_c while the uncertain range is r_e, the target point is $L(x, y)$ and the corresponding node is S_i, and $P_{xy}(P_{xy} = P_{xy}(S_i, d(S_i, L(x, y))))$ denotes the covering probability of S_i to $L(x, y)$. $d(S_i, L(x, y))$ denotes the distance between the location of ith node S_i and the target point $L(x, y)$. Thus, as the simplest case, the deterministic covering model—the boolean model, can be expressed as shown in Eq. (1):

$$P_{xy} = \begin{cases} 1, & d(S_i, L(x, y)) \leq r_c \\ 0, & \text{otherwise} \end{cases} \quad (1)$$

Some other generally adopted probabilistic models are summarized in Table 1.

Table 1: Probabilistic models summary

Name	Functions	Descriptions
Elfes model [37]	$P_{xy} = \begin{cases} 1 & d(S_i, L(x, y)) \leq r_c \\ e^{-\iota(d-r_c)^\kappa} & r_c < d(S_i, L(x, y)) \leq r_c + r_e \\ 0 & \text{otherwise} \end{cases}$	ι and κ are parameters for model adjustment.
Li model [38]	$P_{xy} = \begin{cases} 1 & d(S_i, L(x, y)) \leq r_c \\ e^{-\iota_1(d-r_c)^{\kappa 1}/(r_c+r_e-d)^{\kappa 2}+\iota_2} & r_c < d(S_i, L(x, y)) \leq r_c + r_e \\ 0 & \text{otherwise} \end{cases}$	ι_1, κ_1 and κ_2 are parameters for model adjustment while ι_2 denotes the disturbing effect.
Ahmed multi-layer model [39]	$P_{xy} = \begin{cases} p_1 & d(S_i, L(x, y)) \leq r_1 \\ p_2 & r_1 < d(S_i, L(x, y)) \leq r_2 \\ p_3 & r_2 < d(S_i, L(x, y)) \leq r_3 \\ p_4 & r_3 < d(S_i, L(x, y)) \leq r_4 \\ p_5 & r_4 < d(S_i, L(x, y)) \leq r_5 \\ p_6 & r_5 < d(S_i, L(x, y)) \leq r_6 \\ 0 & \text{otherwise} \end{cases}$	p_1, p_2, p_3, p_4, p_5 and p_6 are the predefined covering probabilities while r_1, r_2, r_3, r_4, r_5 and r_6 are their corresponding covering range thresholds.

(Continued)

Table 1: Continued

Name	Functions	Descriptions
Tsai shadow-fading model [40]	$P_{xy} = Q(10n \lg(d/r_s)/\sigma)$ $Q(x) \triangleq \dfrac{1}{\sqrt{2\pi}} \int_x^\infty e^{-s^2/2} ds$	n ($n \in [2,4]$) denotes the path loss ratio, σ denotes the fading ratio, and r_s is a parameter related to the covering range.
Akbarzadeh sigmoid model [17]	$P_{xy} = 1 - 1/(1 + e^{-\beta(d-r_s)})$	β is a parameter for sensor simulation adjustment.

Finally, for the coverage issue, the power banks are omnidirectional to supply as many sensor nodes as possible, and the FOI is established as a 3-D surface with considering obstacles making it more adaptive for IWSN applications compared to other works in this field [12,41,42]. The problem of NP-hardness in the power bank deployment optimization is overcome with heuristic methods like ABC and its derivatives utilized in the paper, including the proposed approach. Thereafter, by adopting the hybrid power bank deployment model, the optimized power bank deployment locations can be determined and generated.

The rest of the research work is organized as follows; Section two illustrates the methodology employed and discusses the proposed algorithm, general method, and other strategies employed. The experiment conducted is further discussed in section three with comparison experiments, and section four presents the results and analysis. Section five outlines the conclusion of the research work.

2 Methodology

2.1 Formulation of the Problem

The main objective of this research is to design and implement a hybrid power bank deployment model for energy supply coverage optimization in IWSN, which helps prepare the powering supplement of incoming installation of RF-enabled sensor tags. To closely mimic the practical industry environment, the 3-D surface with obstacles is addressed. Although the coverage rate of a particular point is not deterministic once a sensor device of the IWSN is deployed, the coverage probability can be determined according to its physical location and ambient environment. Thus, a combination of the probabilistic coverage model and the line-of-sight algorithm is typically utilized to accurately compute the covering probability of each point on the FOI, which is divided into the covered and uncovered regions accordingly. The critical point is to achieve the optimum coverage of the FOI with a minimum number of power banks, forming the NP-hard deployment problem. While addressing the NP-hard COP, a dynamic search strategy is deployed to balance the ABC algorithm's exploration and exploitation ability, inspired by the differential evolution algorithm. The cellular automata mechanism is further introduced to solve the drawbacks of the proposed heuristic algorithm, simplify the convergence process and accelerate the convergence speed when generating the power bank deployment locations. The research is conducted to achieve optimum coverage of the FOI with a minimum number of power banks operating on RF technology, serving as the source of energy for the installation in the deployment region and minimizing the chances of fires and power outages from direct power sources. The limitation of this paper is that the RF signals are set to operate on the same spectrum. This can be improved upon in future works by expanding the spectrum of propagation to satisfy the various installations in the deployment area. The energy supplied by the RF is of the same capacity, irrespective of the required capacity needed by the installed systems in the deployment area.

Future works would look at satisfying the energy requirement of each installation in the deployment area. The energy of the hybrid power banks can be in a given range from which each device can be powered according to its corresponding capacity.

2.2 Deployment Area

Physical obstacles like machines and manufacturing materials in the deployment area all impact electromagnetic waves' propagation. Instead of ignoring this, we add their interference to the 3-D surface as part of the ambient environment parameter. The 3-D surface model with fluctuation is utilized to mimic the actual environment in the industry as close as possible, as shown in Fig. 2. Due to the fading and shadowing effects of the electromagnetic waves caused by the surrounding obstacles, and the covering range is thus affected. Nevertheless, the surface can be represented by adopting the traditional Cartesian coordinate system for simplicity as $z = f(x, y)$. The coordinates of the nodes must fit the function to verify that it is on the surface and the system. A projecting method to transfer characteristics from the 3-D space to the 2-D ideal plane was also employed to calculate the correlation among them conveniently. The z-projection of a point in the cartesian coordinates at the surface becomes the projection on the x0y plane.

2.3 Covering Model

Due to the existence of obstacles, such as machines and carrier boxes in the production line, the RF energy sent by the power bank can be blocked. In the LOS method, either no obstacles reside between the antenna and the system, or there is a partial obstruction. However, in NLOS, there is a full obstruction between the antenna and the system. For indoor wireless network installations, it is important to consider obstacles such as walls, ceilings, and furniture affecting LOS since these all play a role in wireless signal reception. The utilization of the LOS method is illustrated in Fig. 3.
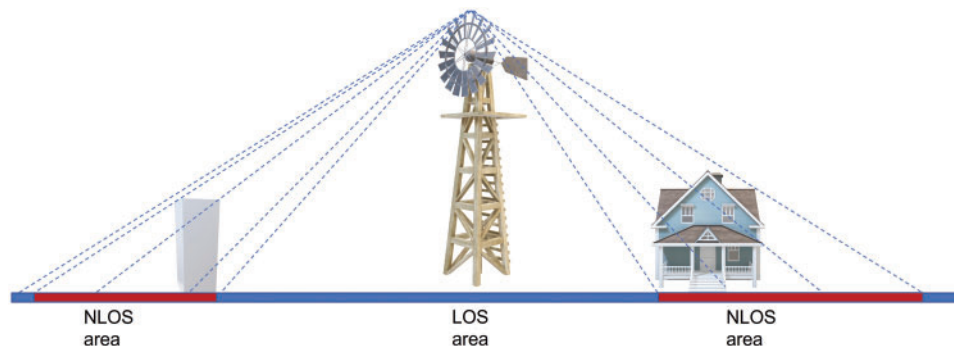
Figure 3: Illustration of LOS and NLOS

A point on the surface is covered only when it is within the range of one or more power banks' coverage. To determine whether each point is on the surface, a probabilistic covering model is utilized to form a mathematical formula considering the characterization of the point coverage rate as a function of distance and other ambient environmental objects.

First, the average coverage range is defined as r_c with an uncertain range r_e. It is natural to assume that $r_e < r_c$. For the point $L(x, y)$ on the surface and its corresponding node S_i, there is a line-of-sight (LOS) when there are no points cut the virtual line draw from N_i to $L(x, y)$. Otherwise, there's no

line-of-sight. Considering the LOS algorithm, the hybrid probabilistic covering model is composed as shown in Eq. (2).

$$P_{xy}\left(S_i, d\left(S_i, L\left(x, y\right)\right)\right) \tag{2}$$

$$= \begin{cases} 1, & r_c - r_e \geq d\left(S_i, L\left(x, y\right)\right) \& LOS \\ e^{-\eta\tau^\varepsilon}, & r_c - r_e < d\left(S_i, L\left(x, y\right)\right) < r_c + r_e \& LOS, \tau \triangleq \dfrac{d\left(S_i, L\left(x, y\right)\right) - \left(r_c - r_e\right)}{2} \\ 0, & r_c + r_e \leq d\left(S_i, L\left(x, y\right)\right) \& NLOS \end{cases}$$

where η and ε define the characteristics of the ambient environment inference on the surface, and $d\left(S_i, L\left(x, y\right)\right)$ is the distance from the node S_i to the point $L\left(x, y\right)$.

Bresenham's algorithm is extended from 2-D to 3-D to differentiate between the node S_i and the point $L\left(x, y\right)$ in the model. The pseudocode is given in Algorithm 1. Thus by comparing the corresponding points with the generated virtual line points, the LOS/NLOS issue can be solved. Given that the two target points on the 3-D surface are specified for the power bank location and a checking point. Then accordingly, without loss of generality, the following assumptions can be made:

$$\begin{cases} \Delta x = x_S - x_L & \Delta x > 0 \\ \Delta y = y_S - y_L & \Delta y > 0, \Delta x = \max\{\Delta x, \Delta y, \Delta z\} \\ \Delta z = z_S - z_L & \Delta z > 0 \end{cases} \tag{3}$$

Assuming the point at $N_{jk}\left(x_j, y_{jk}, z_{jk}\right)$ is determined, the next point to be generated in the column $x_j + 1$ can be determined as:

$$y_{j+1,k} = \begin{cases} y_{jk} + 1 & \varepsilon\left(y_{j+1}\right) \geq 0 \\ y_{jk} & \varepsilon\left(y_{j+1}\right) < 0 \end{cases}, \varepsilon\left(y_{j+1}\right) = y_{j+1} - y_{jk} - 0.5 \tag{4}$$

$$z_{j+1,k} = \begin{cases} z_{jk} + 1 & \varepsilon\left(z_{j+1}\right) \geq 0 \\ z_{jk} & \varepsilon\left(z_{j+1}\right) < 0 \end{cases}, \varepsilon\left(z_{j+1}\right) = z_{j+1} - z_{jk} - 0.5 \tag{5}$$

Next, the optimal location choice for the point $N_{j+1,k}\left(x_j + 1, y_{j+1,k}, z_{j+1,k}\right)$ is among the following 4 locations: $N_{j+1,k}^1\left(x_j + 1, y_{j,k}, z_{j,k}\right)$, $N_{j+1,k}^2\left(x_j + 1, y_{j,k} + 1, z_{j,k}\right)$, $N_{j+1,k}^3\left(x_j + 1, y_{j,k}, z_{j,k} + 1\right)$, $N_{j+1,k}^1\left(x_j + 1, y_{j,k} + 1, z_{j,k} + 1\right)$. Then the parameter for determining the direction at step $i + 1$ can be expressed as:

$$\varepsilon\left(y_{j+2}\right) = y_{j+2} - y_{j+1,k} - 0.5 = \begin{cases} \varepsilon\left(y_{j+1}\right) + k_{yox} - 1 & \varepsilon\left(y_{j+1}\right) \geq 0 \\ \varepsilon\left(y_{j+2}\right) + k_{yox} & \varepsilon\left(y_{j+1}\right) < 0 \end{cases}, k_{yox} = \frac{y_L - y_S}{x_L - x_S} \tag{6}$$

$$\varepsilon\left(z_{j+2}\right) = z_{j+2} - z_{j+1,k} - 0.5 = \begin{cases} \varepsilon\left(z_{j+1}\right) + k_{zox} - 1 & \varepsilon\left(z_{j+1}\right) \geq 0 \\ \varepsilon\left(z_{j+2}\right) + k_{zox} & \varepsilon\left(z_{j+1}\right) < 0 \end{cases}, k_{zox} = \frac{z_L - z_S}{x_L - x_S} \tag{7}$$

These calculations are conducted recursively for each x, starting from the power bank location $N_s\left(x_s, y_s, z_s\right)$. The starting parameters $\varepsilon\left(y_1\right)$, and $\varepsilon\left(z_1\right)$ are evaluated by

$$\varepsilon\left(y_1\right) = y_1 - y_s - 0.5 = k_{yox} - 0.5 \tag{8}$$

$$\varepsilon\left(z_1\right) = z_1 - z_s - 0.5 = k_{zox} - 0.5 \tag{9}$$

As mentioned earlier, the above calculations assume that Δx it is the biggest; thus, Bresenham's algorithm is applied to the projections on the X0Y plane and X0Z plane. The cases for Δy and Δz are likewise.

Algorithm 1: Extended 3-D Bresenham's algorithm

Input power bank location $N_s\,(x_s, y_s, z_s)$ and ending edge location $L\,(x, y)$
Calculate Δx, Δy and Δz
Determine the driving axis by comparing the absolute value of Δx, Δy and Δz
Suppose Δx is the biggest, and X-axis is the driving axis,
$\varepsilon\,(y_0) = 2\Delta y - \Delta x$ and $\varepsilon\,(z_0) = 2\Delta z - \Delta x$
Calculate constants $2\Delta y$, $2\,(\Delta y - \Delta x)$, $2\Delta z$, $2\,(\Delta z - \Delta x)$
Initialize the interpolation's location to $N_s\,(x_s, y_s, z_s)$
Set *cycle* to 1
Repeat
At each x_j along the line, start from $j = 0$, check the transfer conditions for the next point
If $\varepsilon\,(y_j) \geq 0$, then
   Plot $(x_j + 1, y_j, z_j)$ and Set $\varepsilon\,(y_{j+1}) = \varepsilon\,(y_j) + 2\,(\Delta y - \Delta x)$
   Else
      $\varepsilon\,(y_{j+1}) = \varepsilon\,(y_j) + 2\Delta y$
Else if $\varepsilon\,(z_j) \geq 0$, then
   Plot $(x_j, y_j, z_j + 1)$ and Set $\varepsilon\,(z_{j+1}) = \varepsilon\,(z_j) + 2\,(\Delta z - \Delta x)$
   Else
      $\Delta z = 2\Delta z$
$\varepsilon\,(z_{j+1}) = \varepsilon\,(z_j) + 1$
Assign *cycle* = *cycle* + 1
Until (The maximum cycle $\Delta x - 1$ is reached)

After all the above calculations, the FOI is divided into the covered and uncovered regions. The covered area refers to the points covered by one or more power banks, while the uncovered area refers to the points beyond all the power banks' covering range. The uncovered can be visualized as the cavities on the surface and in the quality of network coverage (QoNC) matrix. The DB6 wavelet is adopted to decompose the separable into an approximation image and three detailed images in finding the coverage cavities. Then, by taking the matrix's discrete wavelet transform (DWT) iteratively, the overall QoNC indicates the coverage probability provided by the corresponding power banks at each point.

The QoNC for the FOI can be formulated as:

$$QoNC\,(i) = \frac{1}{m \times n} \sum_{i=1}^{N} \left(\sum_{y=0}^{n} \sum_{x=0}^{m} P_{xy}\,(S_i, d\,(S_i, L\,(x, y))) \right) \tag{10}$$

where i is the number of net nodes on the surface, and $P_{xy}\,(S_i, d\,(S_i, L\,(x, y)))$ is the covering probability in terms of the distance from the node N_i to the point $L\,(x, y)$ in the FOI.

Since many points may be under several nodes' covering range, a scheme is defined when nodes cover a point to modify the probabilistic covering model further to be more accurate. The modified probabilistic covering model is given as:

$$P'_{xy}\,(N_i, d\,(S_i, L\,(x, y))) = 1 - \prod_{i=1}^{\mathbb{N}} \left(1 - P_{xy}\,(S_i, d\,(S_i, L\,(x, y))) \right) \tag{11}$$

After all the computations, the probabilistic coverage index is formed for each point as a matrix. For the QoNC matrix, the values of the element with an index (x_m, y_n) are the covering probability of the point on the surface with the corresponding projecting index $(x_m, y_n, 0)$.

2.4 The Heuristic Algorithms

2.4.1 Motivations for Adopting the Heuristic Algorithms

This research aims to optimize the energy supply coverage regarding the power bank deployment strategy. After the first round of deployment of the power banks, some coverage cavities arise. The problem relates to where the extra power banks can be deployed to fill the cavities while balancing the number of power banks and the overall energy supply coverage rate. The NP-hard problem that forms can be solved by the heuristic algorithm, simulating the natural swarm's working mechanism.

Since we have the model for power net coverage, it is natural that some efforts are made to complete the power net by implementing as few power banks as possible. To better determine the locations of the power banks, the hybrid ABC-DSS with the CA method is adopted to perform the placement optimization.

2.4.2 Overview of the ABC Algorithm

Illuminated by the natural bee swarm's working flow, which mimics the honey bee swarm's forgetting mechanism, Karaboga formulated the ABC algorithm to optimize the numerical functions. The ABC algorithm is a self-organized system with four outstanding characteristics: positive feedback, negative feedback, fluctuations, and multiple interactions, which makes it an attractive group optimization algorithm. A general description of the ABC algorithm is given in Algorithm 2.

Algorithm 2: The artificial bee colony algorithm

Initialize the population x_i and then
Evaluate them
Set *cycle* to 1
Repeat
    For each employed bee
      Produce a new solution v_i
      Compute the fitness
      Utilize the greedy selection process
    For each onlooker bee
      Choose a solution x_i with a probability c_i
      Produce a new solution v_i
      Compute the fitness
      Utilize the greedy selection process
        If there is an abandoned solution for the scout,
         then update with the new solution generated by (12).
    Update the best solution
Assign $cycle = cycle + 1$
Until (Conditions are met or the maximum cycle is reached)

For the ABC algorithm, there is only one employed bee for each food source. The starting point is set as one-half employed bees and the other half onlookers. Each employed bee is randomly nominated

to one source for the first solution. Then by selecting a new candidate solution for each employed bee according to function (12), the employed bee updates its status or not by choosing better fitness acquired from each iteration.

$$v_{ij} = x_{ij} + \theta_{ij}\left(x_{ij} - x_{kj}\right) \tag{12}$$

where j is a random parameter referring to a candidate solution v_i, a current iteration x_i, a neighbour solution x_k, and a random number θ_i ($\theta_i \in [-1, 1]$). To ensure a better candidate with greater chance of being selected, the roulette wheel selection method is adopted to lead the onlooker bee to assess the solution quality while choosing one from them with probability c_i. The definition of fit_i is expressed as shown in (13).

$$c_i = \frac{fit_i}{\sum_{n=1}^{SN} fit_n} \tag{13}$$

When a solution cannot be further improved within a limit parameter, the scout comes out, and a new key will be randomly generated.

$$x_{ij} = x_{j_{\min}} + rand\,(0, 1)\left(x_{j_{\max}} - x_{j_{\min}}\right) \tag{14}$$

where x_i is the solution to be abandoned and D is the dimension of the solution vector while j ($j \in \{1, 2, \cdots, D\}$) is an integer.

2.4.3 Overview of the Modified GABC Algorithm

For group optimization algorithms, the exploration and exploitation ability is vital to the quality of the generated solutions. The former refers to finding the optimum solution in the unknown areas in the solution domain. In contrast, the latter refers to utilizing the experiences gained from previous reasonable solutions to investigate better solutions. However, the exploration ability and the exploitation ability usually conflict with each other in practice. Balancing the two capabilities is essential in achieving a reasonably good optimization.

In the ABC algorithm, as mentioned earlier, the parameter θ_i is a randomly selected number between -1 and 1, which enhances the global search ability while involuntarily ignoring the local search ability and slows the convergence speed. A solving method was proposed in [36] to ease the tension by modifying the searching strategy.

$$v_{ij} = x_{ij} + \phi_{ij}\left(x_{ij} - x_{kj}\right) + \varphi_{ij}\left(y_j - x_{ij}\right) \tag{15}$$

where k, and j are generated in the same manner as in (4), y_j is the jth element of the global best solution, ϕ_{ij} is a random number while $\phi_{ij} \in [-1, 1]$, and φ_{ij} is a uniform random number while $\varphi_{ij} \in [0, C]$, C is a nonnegative constant. Eq. (15) equals Eq. (12) when C equals 0. The ABC algorithm is a particular case of the GABC algorithm. It is proven in [36] that when C equals 1.5, the GABC algorithm performs best. Going over the algorithm, we see that it enhanced the local search ability (exploitation) while protecting the global search ability to a degree. The difference between the ABC algorithm and the GABC algorithm is that Eq. (12) is replaced with Eq. (15).

2.4.4 Overview of the Proposed Modified ABC-DSS Algorithms

Illuminated by the DE algorithm [29], Eq. (15) is rewritten as shown in Eq. (16).

$$v_{ij} = y_j + \theta_{ij}\left(y_j - x_{kj}\right) \tag{16}$$

Analyzing the modified ABC algorithm with Eq. (16), the algorithm has the best solution y_j to guide the search and only yields new solutions around it. Thus, by adopting Eq. (16), the modified ABC Algorithm shortens the computational time to reach convergence and proves its ability in local search. Still, the algorithm easily gets trapped in the local optimum. Since a trade-off between the local search and global search is found while maintaining the convergency time in an acceptable period, a balancing strategy is proposed to perform a compromise between exploration ability and exploitation ability. To combine the two alternatives, a linear parameter α is proposed and defined. From the modality, the parameter will gradually decrease from one to zero along with the searching process, aiming at increasing the weight of y_j while reducing the weight of x_{ij} in the convergence process.

$$\alpha = (Max\_iteration - Current\_iteration)/Max\_iteration \tag{17}$$

To form the dynamic balancing process during the iterations, a self-tuning factor β defined as:

$$\beta = 0.1 \cdot rand\,(0.10) - 0.4 \tag{18}$$

Then the balancing factor λ can be formed as:

$$\lambda = \alpha\beta + 0.4, \lambda \in [0, 1] \tag{19}$$

To avoid premature while escalating the process of convergency, the ABC-DSS is proposed:

$$v_{ij} = \lambda x_{ij} + (1 - \lambda)\,y_j + \theta_{ij}\left(\lambda x_{ij} + (1 - \lambda)\,y_j - x_{kj}\right) \tag{20}$$

Note that when $\lambda = 1$, Eq. (20) equals Eq. (12); when $\lambda = 0$, Eq. (20) equals Eq. (12). The global search ability and convergence efficiency are satisfied by modifying the updating function. The difference between the proposed ABC-DSS algorithm and the ABC algorithm is that Eq. (12) is replaced with Eq. (20).

However, the problem-solving process is not relatively smooth and quick, leading to finding high-order solutions to resolve the problem further. Inspired by the mapping of cellular networks, the FOI is cut into small cells allowing each cell to form the FOI solution accordingly.

The cellular automata (CA), a discrete problem-solving model, is capable of dealing with complex problems while cutting extensive mathematic computations. Since the FOI is a continuous surface in engineering, it is practical to approximate it with discrete space or discrete values. Typically, the CA consists of a regular grid of cells, each assigned a finite number of states, and the grid can be assigned any finite number of dimensions. The four fundamental elements of CA are lattice structure, cell variables, the concept of neighbourhood, and updating rules. In this study, the cells are distributed in each lattice structure, and the neighbouring cells are connected. Adding that the form of the cellular space is the immediate reflection of the physical dimensions, and the rectangular lattice structure is adopted rather than other commonly used triangular and hexagonal lattice structures as the edge shape of the FOI is rectangular. Each cell of the lattice is a joint of parameters that will be updated over the iteration process. The solving process is by defining a set of neighbourhood cells for the specific cell and assigning a random state for each cell to set the initial state. Thus, a new generation is born with the mathematical function that determines the latest state of each cell related to its current state and the states of its neighbouring cells. The cell variables at the time t_{k+1} are:

$$c_l^{k+1} = c_l\,(t_{k+1}) \tag{21}$$

where $c_l\,(t_{k+1})$ is the lth cell variable at time t_{k+1}.

The neighbouring cells n_c of the lth cell are the cell itself and a set of neighbouring cells in the region of the radius r:

$$l - r \leq n_c \leq l + r \tag{22}$$

The configuration of neighbouring cells is a description of the nature of the application, which is vital to the system. The traditional Moore neighbourhood structure [43], which comprises eight cells, is adopted in this article; see Fig. 4.
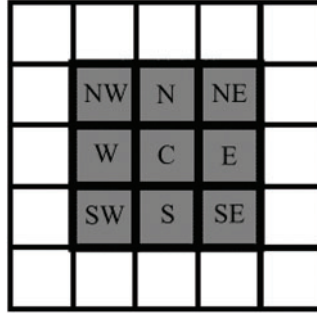
Figure 4: The Moore neighbourhood comprising eight cells

Based on the values needed in the iterations for the updating rules, the updating strategy is:

$$c_l^{k+1} = \Omega\left(c_l^k, c_{n_c}^k\right) = \Omega\left(c_{l-r}^k, \ldots, c_l^k, \ldots, c_{l+r}^k\right) \tag{23}$$

The primary purpose of the ABC-DSS is to seek optimized nectars by exchanging information about the food source position and nectar amount. ABC-DSS-based CA model is introduced to accelerate the convergence speed and derive optimized network topology for WSNs, thus determining the locations of the power banks. In this article, CA is introduced to specify the neighbour solution x_k. The CA method and ABC-DSS method are combined to enhance the optimization search strategy. A new term is added to Eq. (20) based on the CA mechanism to improve the trajectories of particles in the design space. The performance metric of the ABC algorithm lies in the exploration ability, which depends on the interaction between the bees. Utilizing the CA scheme in another way creates a more robust and better interaction for the bees by providing an extra opportunity for the onlooker bees to exchange information with their neighbours. Therefore, the state variables related to each cell are simply the design variables of the optimization problem:

$$c_l \rightarrow X_l^k = x_{kj} \tag{24}$$

The proposed cellular velocity update equation acts on the design variables and combines available information at the central site; thus, for every discrete time step, the updating equation generates a new design at each site using the related information as follows:

$$v_{ij} = \lambda x_{ij} + (1 - \lambda) y_j + \theta_{ij}\left(\lambda x_{ij} + (1 - \lambda) y_j - X_l^k\right) \tag{25}$$

The iteration process is repeated until a stopping criterion is met. The inner and outer loops are regarded as convergent when the limited number of generations in each loop is satisfied.

With all the above modifications, the hybrid power bank deployment model for energy supply coverage optimization is settled, and the optimum power bank deployment locations of a specific FOI are generated.

3 Experimental Studies

3.1 Benchmark Functions

To validate the proposed algorithm and model the COP, the performance of the three algorithms is tested on numerical benchmark function optimizations as was performed in [36], targeting performance evaluation for the heuristic algorithms. The three algorithms are named ABC algorithm, GABC algorithm, and ABC-DSS algorithm, and the benchmark functions used in this research work are shown in Table 2.

**Table 2:** Summary of the benchmark functions

Function name	Functions	Initial range
Sphere	$f_1(x) = \sum_{i=1}^{d} x_i^2$	$[-100, 100]^d$
Griewank	$f_2(x) = \sum_{i=1}^{d} \frac{x_i^2}{4000} - \prod_{i=1}^{d} \cos\left(\frac{x_i}{\sqrt{i}}\right) + 1$	$[-600, 600]^d$
Rastrigin	$f_3(x) = 10d + \sum_{i=1}^{d} \left[x_i^2 - 10\cos(2\pi x_i)\right]$	$[-5.12, 5.12]^d$
Ackley	$f_4(x) =$ $-a\exp\left(-b\sqrt{\frac{1}{d}\sum_{i=1}^{d} x_i^2}\right) - \exp\left(\frac{1}{d}\sum_{i=1}^{d}\cos(cx_i)\right) + a + \exp(1)$ $a = 20, b = 0.2,$ and $c = 2\pi$	$[-32.768, 32.768]^d$
Schwefel	$f_5(x) = 418.9829d - \sum_{i=1}^{d} x_i\left(\sqrt{|x_i|}\right)$	$[-500, 500]^d$
Rosenbrock	$f_6(x) = \sum_{i=1}^{d-1}\left[100\left(x_{i+1} - x_i^2\right)^2 + (x_i - 1)^2\right]$	$[-5, 10]^d$

A set of comparative experiments on the above numerical benchmark function optimizations was conducted to compare the performances of the three algorithms. The dimensions of solution space were set to 30 and 100 for the benchmark function to generate the statistical experiment's means and standard deviation parameters and repeated them 50 times. The population size was set to 80 for all three algorithms, and the maximum generation times were set to 5000.

3.2 Performance Evaluations

The performance of the proposed hybrid power bank deployment model in the industrial environment is evaluated, and the accessibility of powering the energy harvesting in IWSNs is verified in comparative experiments performed on the semi-real 3-D surface. First, to generate the 3D surface with as many features as the natural manufacturing environment, the surface-generate program is coded in MATLAB to represent different environments by setting the parameters at different values. In this paper, the surface models utilized are terrains with narrow and winding canyons, towering and steep mountains named even and uneven plants, as shown in Fig. 5.

After the generation of the 3-D surfaces, the axis of the surface is extracted discretely as the 3D surface is continuous. Bring our assumption to the semi-extreme situation, and the FOI is defined as 2560 meters long and 2560 meters wide, which is a super sizeable single plant according to industry standards. The parameter values set in the simulation are shown in Table 3.

I even plant   II uneven plant
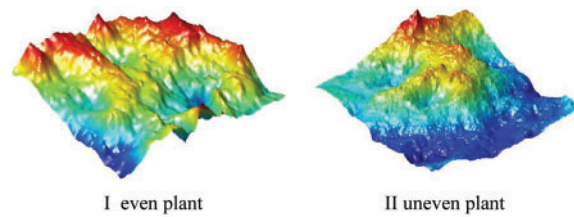
Figure 5: The 3-D generated surfaces

Table 3: The parameter values set in the simulation

Parameter	Quantity	Unit
η	0.1	
ε	2	
m	2560	m
n	2560	m
r_c	55	m
r_u	10	m

4 Results and Analysis

4.1 Experimental Results

Simulation experiments were performed using MATLAB 2022B software to evaluate the proposed algorithm's performance. Six well-known benchmark functions were employed to compare the performance of the ABC, GABC and the ABS-DSS algorithms. Since an absolute 0 may not be reported in practice, and the results below e^{-20} usually function as 0; the values below e^{-20} are treated as 0 in this work. Table 4 shows the optimization values of the mean best fitness and the standard deviation of the Sphere, Griewank, Rastrigin, Akley, Schwefel, and Rosenbrock functions [44–46], respectively. The Sphere function is unimodal, and the others are complex nonlinear multimodal functions. The analysis of variance ANOVA test was performed to evaluate the performance of the proposed algorithm, and compare the results with the other algorithms.

Table 4: Benchmark functions optimized by the ABC, GABC, and ABC-DSS algorithms

Function name	Dimension	Algorithm	Mean best fitness	Standard deviation
Sphere	30	ABC	$7.1935e^{-16}$	$3.403e^{-16}$
		GABC	$4.7661e^{-16}$	$1.802e^{-16}$
		ABC-DSS	$1.2338\ e^{-19}$	$1.532\ e^{-19}$
	100	ABC	$2.9227e^{-9}$	$3.128e^{-10}$
		GABC	$1.8921e^{-9}$	$1.782e^{-10}$
		ABC-DSS	$2.1339e^{-18}$	$3.957\ e^{-19}$
Griewank	30	ABC	$1.5230e^{-15}$	$2.071e^{-15}$
		GABC	$2.9103e^{-18}$	$5.220e^{-18}$

(Continued)

Table 4: Continued

Function name	Dimension	Algorithm	Mean best fitness	Standard deviation
		ABC-DSS	0	0
	100	ABC	$2.6538e^{-10}$	$5.360e^{-10}$
		GABC	$3.9138e^{-16}$	$2.993e^{-16}$
		ABC-DSS	0	0
Rastrigin	30	ABC	$1.4181e^{-14}$	$7.731e^{-15}$
		GABC	$6.2551e^{-17}$	$3.949e^{-17}$
		ABC-DSS	$2.1073e^{-19}$	$2.268e^{-19}$
	100	ABC	$1.9422e^{-7}$	$1.305e^{-6}$
		GABC	$3.3099e^{-11}$	$1.257e^{-11}$
		ABC-DSS	$4.0285e^{-13}$	$2.138e^{-13}$
Ackley	30	ABC	$4.1664e^{-14}$	$5.610e^{-15}$
		GABC	$3.0730e^{-14}$	$2.951e^{-15}$
		ABC-DSS	$2.4857e^{-15}$	$2.874e^{-16}$
	100	ABC	$3.4512e^{-12}$	$1.031e^{-14}$
		GABC	$2.8841e^{-13}$	$6.163e^{-15}$
		ABC-DSS	$1.0008e^{-13}$	$9.131e^{-15}$
Schwefel	30	ABC	$4.0112e^{-4}$	$7.9893e^{-5}$
		GABC	$3.8730e^{-15}$	$9.1651e^{-16}$
		ABC-DSS	0	$2.9878e^{-13}$
	100	ABC	$3.4512e^{-1}$	$1.7905e^{-2}$
		GABC	$2.2463e^{-1}$	$2.9121e^{-2}$
		ABC-DSS	$2.0114e^{-1}$	$4.6071e^{-2}$
	30	ABC	$6.4079e^{-2}$	$5.7493e^{-1}$
		GABC	$2.0761e^{-2}$	$3.2097e^{-1}$
Rosenbrock		ABC-DSS	$1.1761e^{-3}$	0
	100	ABC	$2.1307e^{-1}$	$8.6301e^{-2}$
		GABC	$3.9603e^{-2}$	$3.0814e^{-2}$
		ABC-DSS	$1.8702e^{-2}$	$2.2483e^{-2}$

From Table 4, the proposed ABC-DSS algorithm outperforms the GABC and ABC algorithms for both the unimodal and the multimodal function optimization. More specifically, the ABC algorithm tends to fall into a local optimum, causing convergence stagnation; thus, the convergence accuracy of the algorithm is not ideal. The GABC algorithm strengthened the local search ability with the guidance of the current optimal position of the population; thus, the convergence accuracy of the algorithm improved to a certain extent. Compared with [36,47–49], the proposed ABC-DSS algorithm, kept a good balance between the local and global search ability, is not easily trapped in the numerous local optimal points, and thus has better convergence.

4.2 Performance Evaluation Results

Three strategies are utilized to derive the power bank deployment schemes to address the COP: the ABC-DSS scheme with enabled CA, the ABC-DSS scheme, the GABC scheme, and the ABC scheme. The number of sensors deployed utilizing each scheme is shown in Table 5.

Table 5: The number of power banks deployed in each scheme

3-D surface	Scheme	The number of power banks		
		160 m × 160 m grid size	320 m × 320 m grid size	480 m × 480 m grid size
I	ABC-DSS scheme with enabled CA	1082	916	909
	ABC-DSS scheme	1060	918	913
	GABC scheme	1071	920	914
	ABC scheme	1059	921	917
II	ABC-DSS scheme with enabled CA	929	903	882
	ABC-DSS scheme	926	910	894
	GABC scheme	927	906	889
	ABC scheme	922	911	901

The initial artificial bee number is set as the number of cell grids, and the required QoNC of each cell grid is set to 0.9. The QoNC of each scheme is shown in Table 6.

Table 6: The QoNC of each scheme

3-D surface	Scheme	The number of power banks		
		160 m × 160 m grid size	320 m × 320 m grid size	480 m × 480 m grid size
I	ABC-DSS scheme with enabled CA	0.913879399	0.897543949	0.887221532
	ABC-DSS scheme	0.906251598	0.873535161	0.871670837
	GABC scheme	0.904162738	0.872298720	0.866325168
	ABC scheme	0.903991704	0.871887210	0.859026512
II	ABC-DSS scheme with enabled CA	0.974321732	0.941289353	0.909659437
	ABC-DSS scheme	0.931759837	0.918976599	0.868093241
	GABC scheme	0.930637629	0.917089427	0.867021317
	ABC scheme	0.926214201	0.917056492	0.865903673

The grid size of cells was set at three different degrees to conduct the evaluations; one is 160 meters long plus 160 meters wide, the second is 320 meters long plus 320 meters wide, and the third is 480 meters long plus 480 meters wide. The power bank deployment scheme generating consumption time of each scheme is shown in Table 7.

Table 7: The power bank deployment scheme generating consumption time of each scheme

3-D surface	Scheme	The number of power banks		
		160 m × 160 m grid size	320 m × 320 m grid size	480 m × 480 m grid size
I	ABC-DSS scheme with enabled CA	7.3 min	77.4 min	104.7 min
	ABC-DSS scheme	7.5 min	81 min	131.2 min
	GABC scheme	7.7 min	86 min	142 min
	ABC scheme	8.2 min	88.7 min	147.3 min
II	ABC-DSS scheme with enabled CA	6.4 min	67.3 min	97.6 min
	ABC-DSS scheme	6.7 min	69.8 min	119 min
	GABC scheme	7.5 min	71.9 min	128 min
	ABC scheme	7.7 min	79.6 min	136.9 min

Comparing Tables 5 and 6, we notice that the 160 m × 160 m cell grid scheme results in higher QoNC, although it consumes more power banks. For surface I, Twenty-three power banks are saved between the best and worst schemes while improving the QoNC by 0.01. For surface II, although seven more power banks are utilized between the best and worst scheme, the deployment scheme improved the QoNC by 0.05 and resulted in an extremely high QoNC rate of 0.974. Also, Table 7 shows that the 160 m × 160 m cell grid size scheme consumes less time than the 320 m × 320 m and 480 m × 480 m cell grid size schemes. The time consumed by the 320 m × 320 m cell grid scheme is ten times as long as the 160 m × 160 m cell grid scheme. The reason behind the phenomenon is that the initial artificial bee number was set as the number of cell grids; as a result, the quantity of neighbourhood x_l^k was so large, and the calculation complexity increased to the extent that the optimizing procedure expanded, prolonging the convergence time.

Comparing the ABC-DSS scheme with enabled CA and the ABC-DSS scheme to the ABC scheme in Tables 5 and 6, we can conclude the dynamic search strategy is well balanced in ABC's local and global search abilities to avoid the premature phenomenon. This provides better schemes with higher QoNC. The proposed ABC-DSS scheme with enabled CA scheme outperformed the GABC by 0.01 and the ABC by 0.03 for surface I while surpassing the GABC by 0.04 and the ABC by 0.05 for surface II under 160 m × 160 m cell grid size.

Comparing the ABC-DSS scheme with enabled CA and the ABC-DSS scheme or ABC scheme from Table 7, we can conclude that the CA method helps lower the consumption time of the optimization schemes efficiently. The reason behind the phenomenon is that the CA was utilized to select neighbourhoods in the artificial algorithm other than randomly selecting them, which speeds up the optimization process's convergence.

Since the expected QoNC of the region is 0.9, which was reached by the schemes mentioned above in most cases, the three schemes are verified. However, considering all factors, the ABC-DSS scheme with enabled CA generates better results. Thus, the proposed hybrid power bank deployment model for IWSN is effective and efficient. That is, the FOI is covered as expected, and the energy web can support the operation of the function of the IWSN. The FOI is not defined as the whole area but as

the specified targets or target areas in practice; thus, the QoNC is far beyond 0.9 and could power the entire IWSN.

5 Conclusion

For the COP of WSN and IWSN, traditional research has mainly considered the monitoring coverage of the network and treated the FOI as in a 2-D plane or 3-D space. However, with the booming expansion of printing efficient circuits and fabrication of highly-integrated devices, the application of powering devices by RF is enabled. RF-enabled sensor devices are generally used in industries. Illuminated by the raised issue of widely spreading RF-enabled sensor devices, we focus on the power banks' energy supply coverage in this work. The FOI is not simplified but has considered the obstacles for a more practical 3-D surface. In addressing the NP-hard and COP, modifications were made to the ABC algorithm to generate better and quicker convergence results. A DSS was proposed to modify the ABC and balance the exploration and exploitation ability for better convergence. Further, the CA was utilized to enhance the convergence speed and establish the ABC-DSS with enabled CA. Comparative experiments were carried out for benchmark functions and case studies. The results show that the proposed hybrid power bank deployment model for energy supply coverage optimization in IWSN is effective and efficient.

Based on the limitation of this paper, future works would require that the spectrum of propagation by the RF be expanded to satisfy the various installations in the deployment area. The energy distributed by the power banks can also be varied in the deployment area to satisfy the requirement of each installation.

Conflicts of Interest: The authors declare they have no conflicts of interest to report regarding the present study.

References

[1] J. E. Bresenham, "Algorithm for computer control of a digital plotter," *IBM Systems Journal*, vol. 4, no. 1, pp. 25–30, 1965.

[2] S. W. Nourildean, M. D. Hassib and Y. Mohammed, "Internet of things based wireless sensor network: A review," *Indones. J. Electr. Eng. Comput. Sci.*, vol. 27, no. 1, pp. 246–261, 2022.

[3] R. Ouni and K. Saleem, "Framework for sustainable wireless sensor network based environmental monitoring," *Sustainability*, vol. 14, no. 14, pp. 8356, 2022.

[4] S. Gupta and S. Gupta, "Internet of things and the role of wireless sensor networks in IoT," in *Smart Agricultural Services Using Deep Learning, Big Data, and IoT*. Hershey, USA: IGI Global, pp. 113–127, 2021.

[5] M. J. Nene, R. S. Deodhar and L. M. Patnaik, "Algorithm for autonomous reorganization of mobile wireless camera sensor networks to improve coverage," *IEEE Sensors Journal*, vol. 15, no. 8, pp. 4428–4441, 2015.

[6] C. Han, L. Sun, F. Xiao and J. Guo, "An energy efficiency node scheduling model for spatial-temporal coverage optimization in 3D directional sensor networks," *IEEE Access*, vol. 4, pp. 4408–4419, 2016.

[7] X. Han, X. Cao, E. L. Lloyd and C. -C. Shen, "Deploying directional sensor networks with guaranteed connectivity and coverage," in *2008 5th Annual IEEE Communications Society Conf. on Sensor, Mesh and Ad Hoc Communications and Networks*, San Francisco, CA, USA, pp. 153–160, 2008.

[8] L. C. Shiu, C. Y. Lee and C. S. Yang, "The divide-and-conquer deployment algorithm based on triangles for wireless sensor networks," *IEEE Sensors Journal*, vol. 11, no. 3, pp. 781–790, 2010.

[9]   Y. Zhang, X. Sun and B. Wang, "Efficient algorithm for k-barrier coverage based on integer linear programming," *China Communications*, vol. 13, no. 7, pp. 16–23, 2016.

[10] C. A. R. Soares, R. de Souza Couto, A. Sztajnberg and J. L. M. do Amaral, "POSIMNET-R: An immunologic resilient approach to position routers in industrial wireless sensor networks," *Expert Systems with Applications*, vol. 188, no. 2, pp. 116045, 2022.

[11] R. K. Dash, K. Cengiz, Y. A. Alshehri and N. Alnazzawi, "A new and reliable intelligent model for deployment of sensor nodes for IoT applications," *Computers and Electrical Engineering*, vol. 101, pp. 107959, 2022.

[12] N. H. Ali and R. Özdağ, "Coverage analysis and a new metaheuristic approach using the Elfes probabilistic detection model in wireless sensor networks," *Measurement*, vol. 200, pp. 111627, 2022.

[13] T. Brown, Z. Wang, T. Shan, F. Wang and J. Xue, "On wireless video sensor network deployment for 3D indoor space coverage," in *SoutheastCon 2016*, Norfolk, VA, USA, pp. 1–8, 2016.

[14] H. Ma, X. Zhang and A. Ming, "A coverage-enhancing method for 3D directional sensor networks," in *IEEE INFOCOM 2009*, Rio de Janeiro, Brazil, pp. 2791–2795, 2009.

[15] J. Kumari and P. Kumar, "A spherical band-based DV-Hop localization technique for three-dimensional wireless sensor network," *Physical Communication*, vol. 56, pp. 101945, 2023.

[16] J. Zhang, B. Chen, Y. Zhang, C. Jiang and A. Song, "3D self-deployment of jumping robot sensor nodes for improving network performance in obstacle dense environment," *Measurement*, vol. 207, pp. 112410, 2023.

[17] V. Akbarzadeh, C. Gagne, M. Parizeau, M. Argany and M. A. Mostafavi, "Probabilistic sensing model for sensor placement optimization based on line-of-sight coverage," *IEEE Transactions on Instrumentation and Measurement*, vol. 62, no. 2, pp. 293–303, 2012.

[18] S. Temel, N. Unaldi and O. Kaynak, "On deployment of wireless sensors on 3-D terrains to maximize sensing coverage by utilizing cat swarm optimization with wavelet transform," *IEEE Transactions on Systems, Man, and Cybernetics: Systems*, vol. 44, no. 1, pp. 111–120, 2013.

[19] H. R. Topcuoglu, M. Ermis and M. Sifyan, "Positioning and utilizing sensors on a 3-D terrain part I— Theory and modeling," *IEEE Transactions on Systems, Man, and Cybernetics, Part C (Applications and Reviews)*, vol. 41, no. 3, pp. 376–382, 2010.

[20] J. Yin, N. Deng and J. Zhang, "Wireless sensor network coverage optimization based on Yin-Yang pigeon-inspired optimization algorithm for Internet of Things," *Internet of Things*, vol. 19, no. 8, pp. 100546, 2022.

[21] M. Toloueiashtian, M. Golsorkhtabaramiri and S. Y. B. Rad, "An improved whale optimization algorithm solving the point coverage problem in wireless sensor networks," *Telecommunication Systems*, vol. 79, no. 3, pp. 417–436, 2022.

[22] D. P. Williamson and D. B. Shmoys, *The Design of Approximation Algorithms*, 1st ed., vol. 1. Cambridge, United Kingdom: Cambridge University Press, pp. 3–26, 2011.

[23] J. O'Rourke, "Computational geometry column 15," *International Journal of Computational Geometry and Applications*, vol. 2, no. 2, pp. 215–217, 1992.

[24] J. H. Holland, *Adaptation in Natural and Artificial Systems: An Introductory Analysis with Applications to Biology, Control, and Artificial Intelligence*, 1st ed., vol. 1. Cambridge, MA, USA: MIT press, pp. 171–185, 1992.

[25] J. Kennedy and R. Eberhart, "Particle swarm optimization," in *Proc. of ICNN'95-Int. Conf. on Neural Networks*, Perth, WA, Australia, vol. 4, pp. 1942–1948, 1995.

[26] D. Karaboga, "An idea based on honey bee swarm for numerical optimization," Technical report-tr06, Erciyes university, engineering faculty, computer, 2005.

[27] M. Dorigo and C. Blum, "Ant colony optimization theory: A survey," *Theoretical Computer Science*, vol. 344, no. 2–3, pp. 243–278, 2005.

[28] S. Kirkpatrick, C. D. Gelatt Jr and M. P. Vecchi, "Optimization by simulated annealing," *Science*, vol. 220, no. 4598, pp. 671–680, 1983.

[29] K. Price, R. M. Storn and J. A. Lampinen, "Differential evolution: A practical approach to global optimization," in *Natural Computing Series (NCS)*, 1st ed., vol. 1. Berlin, Germany: Springer Science & Business Media, pp. 189–265, 2006.

[30] D. Karaboga and B. Basturk, "A powerful and efficient algorithm for numerical function optimization: Artificial bee colony (ABC) algorithm," *Journal of Global Optimization*, vol. 39, no. 3, pp. 459–471, 2007.

[31] D. Karaboga and B. Basturk, "On the performance of artificial bee colony (ABC) algorithm," *Applied Soft Computing*, vol. 8, no. 1, pp. 687–697, 2008.

[32] D. Karaboga and B. Akay, "A comparative study of artificial bee colony algorithm," *Applied Mathematics and Computation*, vol. 214, no. 1, pp. 108–132, 2009.

[33] K. -S. Tang, K. -F. Man, S. Kwong and Q. He, "Genetic algorithms and their applications," *IEEE Signal Processing Magazine*, vol. 13, no. 6, pp. 22–37, 1996.

[34] K. Price, R. M. Storn and J. A. Lampinen, *Differential Evolution: A Practical Approach to Global Optimization*. Dordrecht, Netherlands: Springer Science & Business Media, 2006.

[35] R. C. Eberhart, Y. Shi and J. Kennedy, "Swarm intelligence," in *Morgan Kaufmann Series in Evolutionary Computation*, 1st ed., vol. 1. Amsterdam, Netherlands: Elsevier, pp. 287–326, 2001.

[36] G. Zhu and S. Kwong, "Gbest-guided artificial bee colony algorithm for numerical function optimization," *Applied Mathematics and Computation*, vol. 217, no. 7, pp. 3166–3173, 2010.

[37] A. Elfes, "Occupancy grids: A stochastic spatial representation for active robot perception," in *Proc. of the Sixth Conf. on Uncertainty in AI*, Morgan Kaufmann San Mateo, CA, vol. 2929, pp. 6, 1990.

[38] S. Li, C. Xu, W. Pan and Y. Pan, "Sensor deployment optimization for detecting maneuvering targets," in *2005 7th Int. Conf. on Information Fusion*, Philadelphia, PA, USA, vol. 2, pp. 7, 2005.

[39] N. Ahmed, S. S. Kanhere and S. Jha, "Probabilistic coverage in wireless sensor networks," in *The IEEE Conf. on Local Computer Networks 30th Anniversary (LCN'05) l*, Sydney, NSW, Australia, pp. 8–681, 2005.

[40] Y. -R. Tsai, "Sensing coverage for randomly distributed wireless sensor networks in shadowed environments," *IEEE Transactions on Vehicular Technology*, vol. 57, no. 1, pp. 556–564, 2008.

[41] D. Sušanj, D. Pinčić and K. Lenac, "Effective area coverage of 2D and 3D environments with directional and isotropic sensors," *IEEE Access*, vol. 8, pp. 185595–185608, 2020.

[42] J. Liang, M. Tian, Y. Liu and J. Zhou, "Coverage optimization of soil moisture wireless sensor networks based on adaptive Cauchy variant butterfly optimization algorithm," *Scientific Reports*, vol. 12, no. 1, pp. 11687, 2022.

[43] R. Hegselmann and A. Flache, "Understanding complex social dynamics: A plea for cellular automata based modelling," *Journal of Artificial Societies and Social Simulation*, vol. 1, no. 3, pp. 1, 1998.

[44] K. Wójcik, "Forced movement extensions of the particle swarm optimizers with inertia weight," in *Artificial Intelligence and Soft Computing: 21st Int. Conf., ICAISC 2022*, Zakopane, Poland, pp. 254–264, 2022.

[45] R. Ahmed, G. P. Rangaiah, S. Mahadzir, S. Mirjalili, M. H. Hassan *et al.,* "Memory, evolutionary operator, and local search based improved grey wolf optimizer with linear population size reduction technique," *Knowledge-Based Systems*, vol. 264, pp. 110297, 2023.

[46] S. Yang, Y. Qi, R. Yang, X. Ma and H. Zhang, "A surrogate assisted evolutionary multitasking optimization algorithm," *Applied Soft Computing*, vol. 132, pp. 109775, 2023.

[47] H. Shah, N. Tairan, H. Garg and R. Ghazali, "Global gbest guided-artificial bee colony algorithm for numerical function optimization," *Computers*, vol. 7, no. 4, pp. 69, 2018.

[48] Y. Cao, Y. Lu, X. Pan and N. Sun, "An improved global best guided artificial bee colony algorithm for continuous optimization problems," *Cluster Computing*, vol. 22, pp. 3011–3019, 2019.

[49] X. Ruan, J. Wang, X. Zhang, W. Liu and X. Fu, "A novel optimization algorithm combing Gbest-guided artificial bee colony algorithm with variable gradients," *Applied Sciences*, vol. 10, no. 10, pp. 3352, 2020.